J Electroceram (2007) 19:375–381
DOI 10.1007/s10832-007-9176-5

Ultrasonic transducer based on highly textured PMN-PT piezoelectric ceramic

F. Levassort · M. Pham Thi · P. Marechal · L.-P. Tran-Huu-Hue · M. Lethiecq

Received: 6 March 2006 / Accepted: 14 May 2007 / Published online: 13 June 2007

Abstract A successful fabrication process of textured ceramics by homo-template grain growth (HTGG) is described. Two samples fabricated with this technique were characterised. Functional properties obtained are competitive with for example a thickness coupling factor over 50%. Different characteristics were compared with those obtained by a unit cell model previously developed for piezocomposites and extended to the case of two piezoelectric phases. Behaviours of several connectivities (0–3, 3–0 and 3–3) are calculated and results show that the spatial arrangement does not have a great influence on effective parameters. A transducer based on a textured ceramic sample has been fabricated and characterised. The measured performance shows the efficiency of these new piezoelectric materials. Finally, electroacoustic responses of identical single element transducer configurations have been simulated. They show that a sensitivity increase of 3dB can be obtained at equivalent relative bandwidth of 40% with textured ceramic sample in comparison with PMN-PT ceramic used as a matrix in the textured ceramic.

Keywords Textured ceramic · Piezoelectricity · Ultrasonic transducer

F. Levassort (✉) · P. Marechal · L.-P. Tran-Huu-Hue · M. Lethiecq
Francois Rabelais University LUSSI,
10 boulevard Tonnellé, BP 3223, 37032 Tours cedex 1, France
e-mail: levassort@univ-tours.fr

M. P. Thi
Thales Research & Technology,
128 Route Départementale,
91767 Palaiseau cedex, France

1 Introduction

The association of several materials having different properties (e.g. elastic, dielectric,...) has allowed to combine several advantages of constitutive material that no single constituent can deliver. This principle has been applied to piezoelectric materials at the end of 1970s by Newnham et al. [1] where the concept of connectivity to classify the spatial arrangement between phases in a piezocomposite has been introduced. This concept can be extended, with several assumptions, to the case of two piezoelectric phases such as in textured ceramics. Piezoelectric single crystals (such as PZN-9%PT or PMN-32%PT) are largely studied because of very high electromechanical coupling factors, but the fabrication in large dimensions with constant properties is difficult which is an important issue for transducer fabrication. A trade-off can be found with highly oriented ceramics where electromechanical properties can approach those of oriented single crystals. The fabrication of such materials in large dimensions is possible with the process used here.

In the following section, the fabrication process of textured PMN-PT ceramics obtained by homo-template grain growth (HTGG) will be described. The fabricated samples have electromechanical properties between those of the two constitutive materials (polycrystalline PMN-35% PT and single crystal templates PMN-25%PT). Behaviour of the dielectric losses as a function of frequency is also discussed.

The modelling of an inhomogeneous media (where the properties are constant in each phase) as a homogeneous material which is characterised by a single set of effective constants merged in electroelastic moduli for piezoelectric materials is known as a homogenisation method. Such

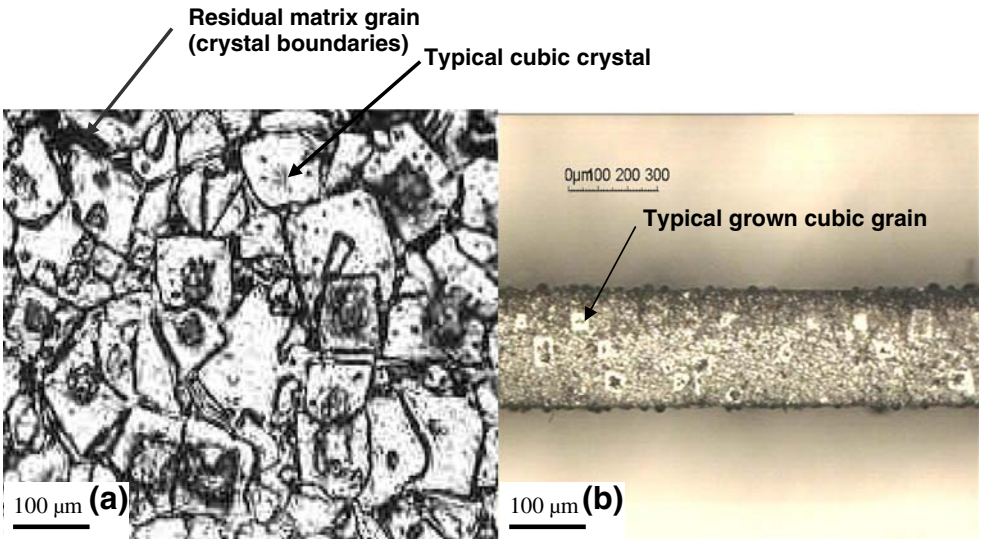

Fig. 1 Optical microphotographs of PMN-PT textured ceramics displaying texture fraction of 0.95, recorded on as-sintered surface (**a**), and polished sample, displaying texture fraction of 0.7 cut perpendicular to the disk surface (**b**)

modelling requires all the properties of each phase, their geometries, morphologies (size, form, orientation, distribution) to be known. All these characteristics are very difficult to obtain simultaneously and a majority of models assumes that the overall average is replaced by a volume average on a representative elementary volume which is small in comparison with the sample and large with regard to the microstructure. The model used in Section 3 is based on this hypothesis. Additional assumptions and restrictions related to the textured ceramics are also specified. Several effective parameters are calculated for three connectivities and compared with experimental results.

With a textured ceramic sample, a simple ultrasonic transducer has been fabricated and characterised. Finally, to quantify the interest of using textured ceramic, several simulations of electro-acoustic responses of standard single-element transducers with the KLM scheme [2] have been performed with different piezoelectric materials.

2 Fabrication process

PMN-PT relaxor textured ceramics were prepared by in situ template grain growth with tape casting [3, 4]. Seeds in the shape of $(1-x)$PMN$-x$PT cubic single crystals with composition close to $x=0.25$ were obtained by the flux method. Perfect cubic crystals of $50\times50\times50$ μm^3 were selected as templates.

Nanosized $(1-x)$PMN-xPT:Mn perovskite matrix powder ($x=0.35$) was first prepared by solid-state reaction via Columbite method and then milled using continuous attrition milling with micro beads. Nanosized PMN-PT: Mn powders exhibiting the BET surface areas of 12–20 m^2/g and 5 wt% of templates were mixed with organic binder to obtain homogenous slurry (initial proportion of nanopowder is 60 wt% in the organic binder). The mixture was tape cast using the doctor blade technique to obtain tapes of 150 μm thick. Orientation of the templates was obtained during tape

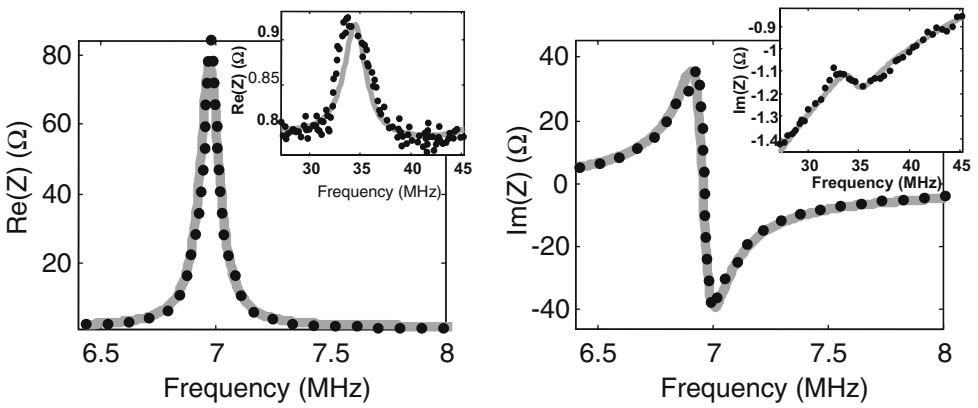

Fig. 2 Electrical impedance of the textured ceramic sample 1 around f_a and at the 5th overtone (*black points*: experimental values; *grey solid lines*: theoretical values)

Table 1 Characteristics of two textured ceramic samples.

Sample	A (mm^2)	f	V_f (%)	ρ (kg m^{-3})	f_a (MHz)	v_l (m s^{-1})	k_t (%)	$\varepsilon_{33}^S/\varepsilon_0$	δ_m (%)
1	124	0.6	30	8,060	6.9	4,580	51	1,305	1.8
2	124	0.7	40	8,060	5.9	4,500	49	1,400	5.1

A, electrode area; f, Lotgering factor; V_f, single crystal volume fraction; ρ, density; f_a, anti-resonant frequency; v_l, longitudinal wave velocity; k_t, thickness mode coupling factor; $\varepsilon_{33}^S/\varepsilon_0$, dielectric constant at constant strain measured at f_a; δ_m, mechanical loss factor.

casting. Green tapes were dried, stacked, laminated and cut into disks (diameter of 16 mm, thickness of 0.5 to 1 mm). Tape stacks were sintered between 1150 and 1200°C for different durations under O_2 in PbO-rich atmosphere. All ceramics exhibit a density in the range 93–95%.

Orientation and microstructure of PMN-35%PT textured ceramic were investigated by X-ray diffraction spectra (XRD) and optical spectroscopy. XRD spectra, recorded on raw and polished ceramic surface exhibit an intensity increase of the (00l) diffraction peaks revealing the orientation of PMN-PT ceramics. A <001> texture fraction of PMN-PT tape cast textured ceramic was estimated by the Lotgering method from spectra recorded with $\theta/2\theta$ X-ray using a Seifert MZ-IV goniometer in the Bragg-Brentano geometry. The Lotgering factor (f) describes the degree of texture of the scanned surface area.

Depending on sintering conditions, textured tape cast ceramics display a texture fraction from 0.3 to quasi complete (001) texture (f=0.95) in the cubic phase. The orientation relationship [5] between grains was investigated by a ω-scan of the {001} peak recorded on polished surface. The full width at half maximum (FWHM) of the peak is equal to 9° and 6° for samples displaying texture of 0.7 and 0.96, respectively. Therefore, we can conclude that orientation distribution of {001} direction in textured ceramics is very small and out of plane alignment is good.

Optical microphotograph (Fig. 1a) of the sample, displaying f=0.95, reveals a nearly complete pavement of cubic crystals with residual matrix grains at the crystal boundaries. The growth area around the pristine crystal templates can be clearly observed: crystal cores appear in black and the periphery in white [6]. It is important to note that the analysed surface is about ~1 cm^2 and the penetration depth of X-ray at 20–40 keV is a few microns. The texture fraction was determined on a polished surface sample and, for that, approximately 100 μm thick of ceramic was removed. The Lotgering factor measured on the polished surface is equal to that obtained from the as-sintered surface. Optical micrographs (Fig. 1b) of a sample, cut perpendicular to the disc surface show large grown cubic grains. The initial green ceramic layers could easily be observed by the superposition of grown cubic grains in the ceramic thickness. Thus, the orientation of ceramic matrix along the (001) axis was obtained in all considered volumes.

3 Functional characterisation and modelling

3.1 Characterisation

Two textured ceramic discs with different Lotgering factors have been characterised to deduce properties related to the thickness mode. Using the geometrical characteristics (electrode area and thickness) and the density of the different samples, a fit of the experimental electrical impedance of a piezoelectric element in free resonator conditions [7] allows to determine other parameters. The experimental set-up is composed of a HP4395A impedance analyser and its impedance test kit with a spring clip-fixture where the piezoelectric samples are placed under free resonator conditions. Complex electrical impedance curves of one of the two samples are represented in Fig. 2 around the fundamental resonance and also at the 5th overtone. All the parameters deduced are given in Table 1. The two samples have a thickness coupling factor around 50% which is higher than that of standard PZT ceramics.

Moreover, measurements have been performed on two overtones (the 3rd and 5th) on one sample (number 1; see Fig. 2 for the 5th overtone). Using these fits, the behaviour of mechanical losses as a function of frequency (between 6 and 34 MHz) has been deduced. If a linear dependence is assumed, the variation of 3.1×10^{-3} MHz^{-1} is obtained.

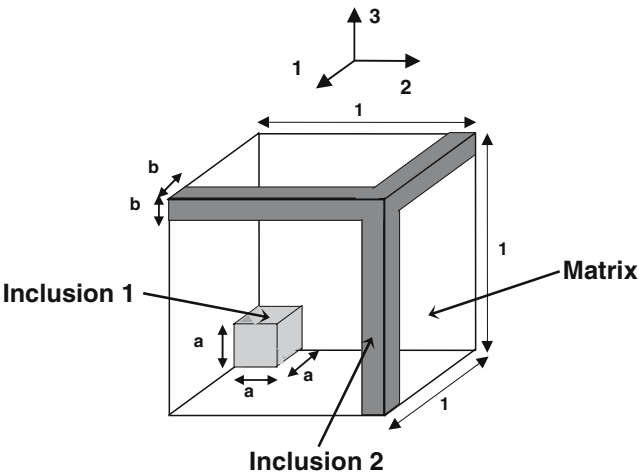

Fig. 3 Definitions of the unit cell with different connectivities for textured ceramics. Coordinate system is added (*3*: poling direction)

Table 2 Characteristics of PMN-35%PT ceramic and PMN-PT single crystal.

Material	ρ (kg m^{-3})	v_l (m s^{-1})	k_t (%)	$\varepsilon_{33}^S/\varepsilon_0$
PMN-35PT	8,060	4,740	43	2,650
PMN-PT SC	8,060	4,610	62	925

ρ, density; v_l, longitudinal wave velocity; k_t, thickness mode coupling factor; $\varepsilon_{33}^S/\varepsilon_0$, dielectric constant at constant strain measured at f_a.

This slope is relatively high in comparison with those measured on a standard PZT (7×10^{-4} MHz^{-1} for Ferroperm Pz27) [8] and on single crystals in which losses are quasi-constant [9]. The heterogeneity of the microstructure in textured ceramics (as shown in Fig. 1) probably contributes to increase the mechanical losses.

3.2 Modelling

A textured ceramic can be described by a unit cubic cell where one phase is represented by a single inclusion in the rest of the cell (matrix). The spatial arrangement between the two phases changes the effective properties of the composite material. With this modelling, the shape of the single inclusion can be easily adapted to change the connectivity [1]. In the Fig. 3, if only inclusion 1 is considered the cell represents the 0–3 connectivity where the properties of the inclusion are those of the single crystal and the properties of the matrix are those of the polycrystalline PMN-PT ceramic. For the 3–0 connectivity, the properties of the inclusion and those of the matrix are simply switched. If the inclusion 2 is now considered alone in the cell, the 3–3 connectivity can be modelled. Electroelastic moduli of the textured ceramics are calculated as a function of single crystal volume fraction for each of these

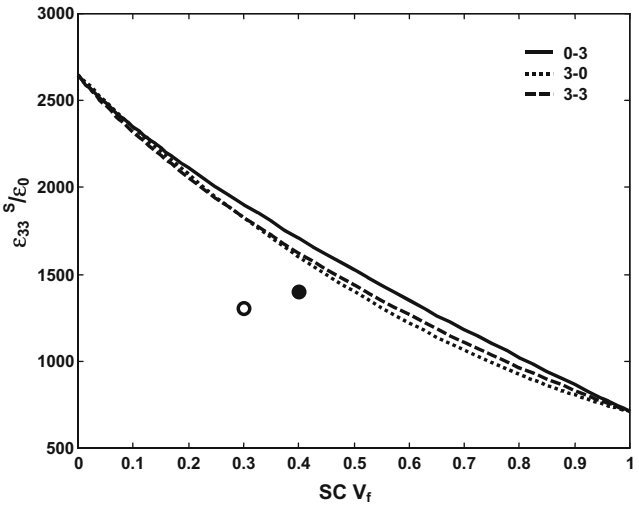

Fig. 4 Dielectric constant at constant strain ($\varepsilon_{33}{}^S/\varepsilon_0$) as a function of single crystal volume fraction for three connectivities. Experimental data is added (*hollow circle*: sample 1, *solid circle*: sample 2 from Table 1)

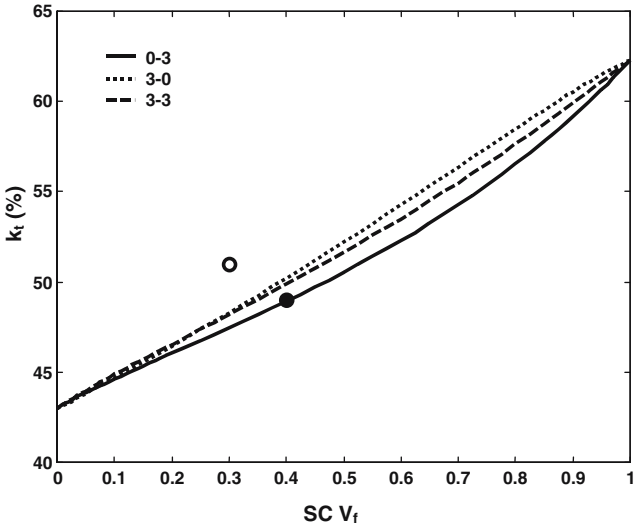

Fig. 5 Electromechanical coupling factor in thickness mode (k_t) as a function of single crystal volume fraction for three connectivities. Experimental data is added (*hollow circle*: sample 1, *solid circle*: sample 2 from Table 1)

connectivities. For this, the values a and b (Fig. 3) are easily related to the volume fraction of single crystal in the material. The different steps for the calculation are detailed in [10, 11]. A generalisation of the series and parallel analysis developed for 2–2 connectivity (stack of alternative layers of single crystal and ceramic) with a matrix resolution is used. The cell described in Fig. 3 is decomposed in blocks where each block corresponds to an intermediate material in 2–2 (or 1–3) connectivity. Between the two phases, rigid boundaries are assumed and anisotropy of the effective electroelastic moduli is similar to that of the single crystal phase.

This modelling assumes that only two phases with constant properties co-exist in the material whatever the volume fraction of single crystal. Two compounds have clearly been distinguished by XRD analysis [5, 12]. Moreover, the orientation distribution in textured piezoelectric polycrystal is not taken into account [13] but using XRD analysis, a low orientation distribution is observed on the samples studied here, as mentioned in Section 2.

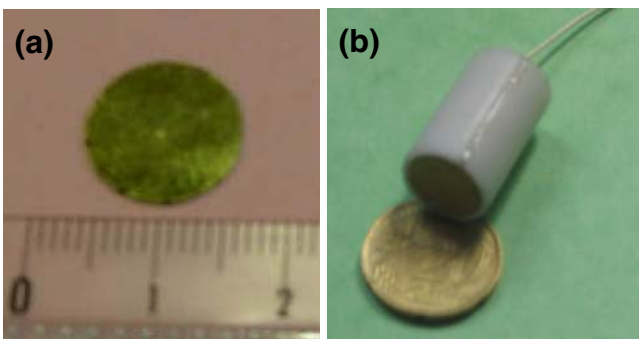

Fig. 6 Photographies of (**a**) textured ceramic sample (*number 1*); (**b**) transducer based on textured ceramic sample (*number 2*)

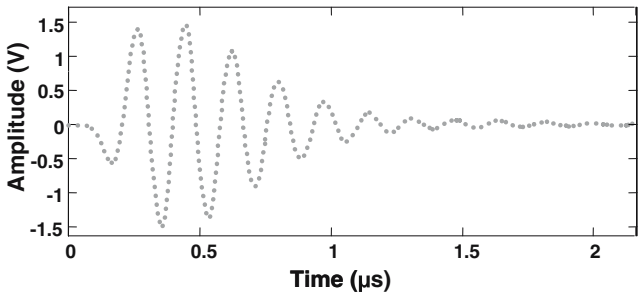

Fig. 7 Experimental electroacoustic response of the transducer integrating a textured ceramic sample (*number 2*)

Simulation of effective properties of the textured ceramic requires the knowledge of material constants of the two phases (PMN-PT single crystal and ceramic). Unfortunately, electroelastic moduli of single crystal cubic templates with typical sizes between 50 and 100 μm for the side are not available. Published data on a material with close composition (PMN-29%PT) measured on larger samples is used [4, 14]. Moreover, a self-consistence between tensor components is necessary for the modelling and complete data of PMN-33%PT has been used [15, 16]. For the random ceramic (PMN-35%PT), standard characterisations with several samples having different geometries have been used [4, 17]. According to all the component tensors of the two phases, a few parameters such as the thickness coupling factor and the longitudinal wave velocities are deduced and given in Table 2.

As mentioned in Section 2, the Lotgering factor has been used to quantify the degree of oriented structure at room temperature with a non-destructive X-ray diffraction method [5]. The single crystal volume fraction is used as a key parameter in the modelling. For several textured ceramic samples, relation between the Lotgering factor values and volume fractions of single crystal phase in samples has been studied. For this, imaging analysis has been performed on the surface of samples to calculate the percentage of single crystal material and due to good homogeneity in the volume of single crystal distribution (observed on cross section sample, Fig. 1b), a non-linear relation has been extended to the volume fraction. In Table 1, and using this relation, volume fractions of single crystal have been deduced from the Lotgering factor for the two samples.

Figures 4 and 5 represent evolutions of the dielectric constant at constant strain and thickness coupling factor as a function of single crystal volume fraction (SC V_f) for three simulated connectivities (0–3, 3–0 and 3–3). Results show that small variations appear between the connectivities and so the arrangement between phase does not seem to be predominant for the effective properties, contrary to piezocomposites based on one piezoelectric phase and one inert phase (typically a polymer) [11]. These results show clearly that in all cases, a high volume fraction of single crystal and consequently a high degree of texturing is essential to significantly increase the performance (in particular the thickness coupling factor which represents the major parameter to deliver high transducer performance) of the textured piezoelectric ceramics. In Fig. 4, experimental values of the two samples are found to be lower than the predictions. The main explanation can be the porosity which has been observed in the samples but not taken into account in the modelling. This porosity tends to decrease the dielectric constant and the corresponding value is probably higher in sample 1 than in sample 2. For the thickness coupling factors (Fig. 5), values measured for the two samples are in the same order as the predictions but uncertainties in the input data have a significant effect.

4 Ultrasonic transducers

4.1 Fabricated transducer

The main objective of the transducer fabrication described in this paragraph is to demonstrate the feasibility and competitive performance of the textured ceramic sample. Consequently, an arbitrary transducer backing has been chosen. A simple transducer composed of a backing made with epoxy resin loaded with metallic particles (the corresponding acoustical impedance is 8 MRa) and the textured ceramic sample 2 has been manufactured. No matching layer has been added. Electrical contacts on the front and rear gold

Table 3 Characteristics of the three simulated transducers.

	Material in transducer	Z_p (MRa)	Z_b (MRa)	Z_l (MRa)	e_p (μm)	e_l (μm)	BW(−6 dB; %)	BW(−20 dB; %)	IL (dB)
1	PMN-PT SC	37.2	6.5	4.0	325	76	44	80	0
2	Sample 1	37.5	6.5	4.3	330	73	40	73	−3
3	PMN-35PT	38.2	6.5	4.4	345	75	39	70	−6

Z_p, acoustical impedance of the piezoelectric element; Z_b, acoustical impedance of the backing; Z_l, acoustical impedance of the matching layer; e_p, thickness of the piezoelectric element; e_l, thickness of the matching layer; BW(−6dB), relative bandwidth at −6 dB; BW(−20 dB), relative bandwidth at −20 dB: IL, insertion loss (normalised with single crystal transducer).

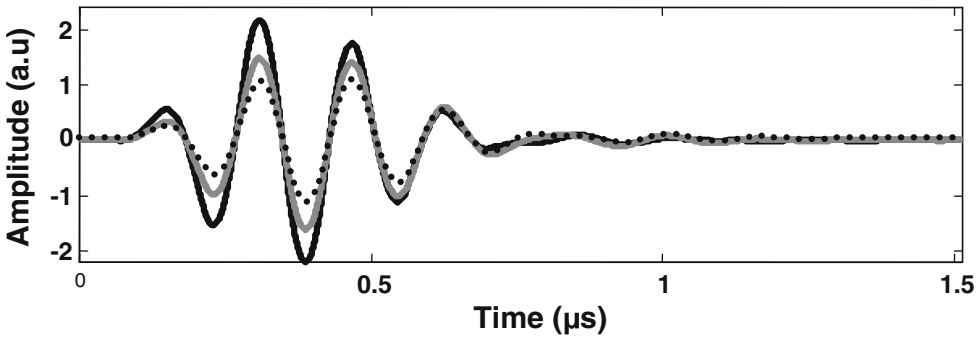

Fig. 8 Superimposition of simulated electro-acoustic responses of three transducers with the same centre frequency (6.4 MHz) based on textured ceramic (sample number 1, *grey solid line*), PMN-PT ceramic (*black points*), PMN-PT single crystal (*black solid line*)

electrodes of the piezoelectric disc have been made and the two elements have been put in an insulating housing. Photographs of the textured ceramic disk and transducer using this element are shown in Fig. 6. The electro-acoustic response measured in a water tank on a metallic target is represented in Fig. 7. The centre frequency is at 5.5 MHz and the bandwidths deduced respectively at −6dB et −20 dB are found to be 29 and 100%. This result demonstrates large possibilities of applications of textured ceramics.

4.2 Results and comparison

To compare more precisely the performance of a transducer based on piezoelectric textured ceramic, the KLM scheme [2, 18] has been used to calculate the electro-acoustic responses and corresponding properties of three transducers composed of a backing with the same acoustical impedance (6.5 MRa), a piezoelectric element and a matching layer adapted to a water propagation. The first and third transducers used respectively the properties of the PMN-PT single crystal and PMN-PT ceramic for the piezoelectric element (Table 2). The second transducer used the properties of the textured ceramic sample (number 1, Table 1). For these simulations, the dielectric constant being different between piezoelectric materials, the transducer performance has been calculated independently of electrical environment. The centre frequency is the same in the three cases and has been fixed by the thickness of the textured ceramic sample. For the two other ones, the thickness has been adjusted to keep a value of 6.4 MHz. Finally, an optimisation approach has been used to calculate the thickness and acoustical impedance of the matching layers [19]. This method defines a performance index (PI) composed of sensitivity and bandwidth parameters of the transducer. The weighting of each parameter in the PI depends on the application (here for medical imaging [20]). The transducer parameters and then the PI are calculated from the electro-acoustic response obtained with the KLM scheme. In minimising the PI, the matching layer parameters are deduced. Table 3 summarises the data obtained and Fig. 8 gives the superimposition of the three corresponding electro-acoustic responses. The large difference between the thickness coupling factors of the PMN-PT single crystal and ceramic delivered a variation of 6 dB of the sensitivity and also a slight increase of the bandwidth. Logically, intermediate results are obtained for the second transducer with a sensitivity 3 dB higher in comparison with the third transducer. Finally, a margin remains for the textured ceramic, since by further increasing the degree of texture, another 3 dB could be gained.

5 Conclusion

Fabrication of piezoelectric ceramics by homo-template grain growth was briefly recalled. Two samples with different degrees of texture were characterised (microstructure and functional properties). Experimental results were compared to a model previously developed for piezocomposites with one inert phase which is here extended to two piezoelectric phases. Several additional studies will be necessary to improve the modelling, in particular taking into account the effect of porosity in the samples on the effective parameters. Moreover, the poling step has a large influence on electromechanical properties and optimisation in the fabrication process will also be an important point to increase performance. At this stage, measured electromechanical properties are already higher than those of standard PZT or PMN-PT ceramics with for example a thickness coupling factor over 50%. These encouraging results have been confirmed through the fabrication of a first transducer based on textured ceramic sample and through simulations of electro-acoustic responses of different transducers with same centre frequency. Results show that at equivalent −6 dB relative bandwidth (40%), sensitivity using textured ceramic is increased by 3 dB in comparison with a transducer integrating a PMN-PT ceramic disc which has the same properties as the initial matrix of the textured ceramic.

Acknowledgement This work was performed in the frame of the PIRAMID FP5 European project, contract No. G5RD-CT-2001-456. The authors would like to thank Marion Bailly for transducer manufacturing.

References

1. R.E. Newnham, D.P. Skinner, L.E. Cross, Connectivity and piezoelectric-pyroelectric composites. Mater. Res. Bull. **13**, 525–536 (1978)
2. R. Krimholtz, D.A. Leedom, G.L. Matthei, New equivalent circuit for elementary piezoelectric transducers. Electron. Lett. **38**, 338–339 (1970)
3. M. Pham Thi, H. Hemery, Homoepitaxial Template Grain Growth of Textured PMN-PT ceramics. CIMTEC, 10th International Ceramics Congress, Part. **631** (2002)
4. H. Hemery, Céramiques orientées hautes performances: Pb(Mg1/3Ng2/3)03-PbTiO3 par croissance pseudo-morphose. INSA Lyon France, (2003) Ph.D Thesis (In French)
5. M. Pham Thi, H. Hemery, O. Durand, H. Dammak, Orientation distribution and fiber textured of highly oriented piezoceramics: (1-x)PbMg1/3Ng2/303 -xPbTiO3 system. J. J. Appl. Phys. **43**(12), 8190 (2004)
6. M. Pham Thi, G. March, P. Colomban, Phase diagram and raman imaging of grain growth mechanism in highly textured Pb(Mg1/3Nb 1/3)O3-PbTiO3 piezoelectric ceramics. J. Eur. Ceram. Soc. **25**(14), 3335 (2005)
7. D. Royer, E. Dieulesaint, Ondes elastiques dans les solides. Tome 1: Propagation libre et guidée. Masson Ed. (1996)
8. L.P. Tran-Huu-Hue, F. Levassort, N. Felix, D. Damjanovic, W. Wolny, M. Lethiecq, Comparison of several methods to characterize the high frequency behavior of piezoelectric ceramics for transducer applications. Ultrasonics **38**(1), 219–223 (2000)
9. T. Delaunay, E. Le Clézio, H. Dammak, P. Gaucher, M. Pham Thi, M. Lethiecq, G. Feuillard, Frequency dependence of electromechanical properties of PZN-xPT single crystals. J. Phys. IV. **128**, 161–167 (2005)
10. F. Levassort, M. Lethiecq, D. Certon, F. Patat, A matrix method for modeling electroelastic moduli of 0–3 piezo-composites. IEEE Trans. Ultrason. Ferroelect. Freq. Control. **44**(2) 445–452 (1997)
11. F. Levassort, M. Lethiecq, R. Desmare, L.P. Tran-Huu-Hue, Effective electroelastic moduli of 3–3(0–3) piezocomposites. IEEE Trans. Ultrason. Ferroelect. Freq. Control. **46**(4), 1028–1034 (1999)
12. M. Pham Thi, H. Hemery, H. Dammak, X ray investigation of high oriented (1-x)PbMg1/3Ng2/303-(x)PbTiO3 ceramics. J. Eur. Ceram. Soc. **25**, 2433–2435 (2005)
13. J.Y. Li, The effective electroelastic moduli of textured piezoelectric polycristalline aggregates. J. Mech. Phys. Solids. **48**, 529–552 (2000)
14. W. Jiang, Z. Zhang, B. Jiang, W. Cao, Characterisation of piezoelectric materials with large piezoelectric and electromechanical coupling coefficients. Ultrasonics. **41**, 55–63 (2003)
15. R. Zhang, B. Jiang, W. Cao, Elastic, piezoelectric and dielectric properties of multidomain 0.67Pb(Mg1/3Nb2/3)O3-0.33PbTiO3 single crystals. J. Appl. Phys. **90**(7), 3471–3475 (2001)
16. R. Zhang, B. Jiang, W. Cao, Orientation dependence of piezoelectric properties of single domain 0.67Pb(Mg1/3Nb2/3)O3-0.33PbTiO3 crystals. Appl. Phys. Lett. **82**(21), 3737–3739 (2003)
17. IEEE Std., Standard on Piezoelectricity ANSI/IEEE Std. 176-1987. IEEE Trans. Ultrason. Ferroelect. Freq. Control **43**(5), 719–772 (1996)
18. S.J.H. Van Kervel, J.M. Thijssen, A calculation scheme for the optimum design of ultrasonic transducers. Ultrasonics **21**, 134–140 (1983)
19. R. Desmare, L.P. Tran-Huu-Hue, F. Levassort, M. Lethiecq, Optimisation method for ultrasonic transducers used in medical imaging. Journal Revista de Acustica. **33**, (2003)
20. J.M. Thijssen, W.A. Verhoef, M.J. Cloostermans, Optimisation of ultrasonic transducers. Ultrasonics 41–46 (1985)